COMPARING DIRECT CARBONATE and STANDARD GRAPHITE 14C DETERMINATIONS of BIOGENIC CARBONATES

(Article begins on next page)

25 April 2024

1   **Comparing direct carbonate and standard graphite ^{14}C determinations from an assortment**

2   **of biogenic carbonates**

3

4   Jordon Bright[1*], Chris Ebert[2], Matthew A. Kosnik[3], Darrell S. Kaufman[1], Katherine Whitacre[1],

5   John R. Southon[4], Paolo G. Albano[5], Carola Flores[6,7], Thomas K. Frazer[8], Quan Hua[9], Michal

6   Kowalewski[10], Julieta C. Martinelli[11], David Oakley[12], Wesley G. Parker[13], Michael Retelle[14],

7   Matias do Nascimento Ritter[15], Marcelo M. Rivadeneira[6,7,16], Daniele Scarponi[17], Yurena

8   Yanes[13], Martin Zuschin[5]

9

10   [1] School of Earth and Sustainability, Northern Arizona University, Flagstaff, AZ, 86011, USA

11   [2] Center for Ecosystem Sciences and Society, and Department of Biological Sciences, Northern

12   Arizona University, Flagstaff, AZ, 86011, USA

13   [3] Department of Biological Sciences, Macquarie University, New South Wales 2109, Australia

14   [4] Keck Carbon Cycle AMS Laboratory, Department of Earth System Science, University of

15   California at Irvine, Irvine, CA 92697, USA

16   [5] Department of Paleontology, University of Vienna, Althanstrasse 14, Vienna, Austria

17   [6] Centro de Estudios Avanzados en Zonas Áridas (CEAZA), Av. Ossandón 877, C.P. 1781681,

18   Coquimbo, Chile

19   [7]Departmento de Biología Marina, Facultad de Ciencias del Mar, Universidad Católica del

20   Norte, Av. Larrondo 1281, Coquimbo, Chile

21   [8] School of Natural Resources and Environment, University of Florida, Gainesville, FL, 32611,

22   USA

1

23   [9] Australian Nuclear Science and Technology Organisation, Locked Bag 2001, Kirrawee DC,

24   NSW 2232, Australia

25   [10] Florida Museum of Natural History, University of Florida, Gainesville, FL, 32611, USA

26   [11] School of Fishery and Aquatic Sciences, University of Washington, Seattle, WA, 98105, USA

27   [12] Department of Geosciences, Pennsylvania State University, University Park, PA, 16802, USA

28   [13] Department of Geology, University of Cincinnati, Cincinnati, OH, 45221, USA

29   [14] Department of Geology, Bates University, Lewiston, ME, 04240, USA

30   [15] Centro de Estudos Costeiros, Limnológicos e Marinhos, Campus Litoral Norte, Universidade

31   Federal do Rio Grande do Sul, Imbé, 95625-00, Rio Grande do Sul, Brazil

32   [16] Departmento de Biología, Universidad de la Serena, Av. Raul Bitrán 1305, La Serena, Chile

33   [17] Department of Biological, Geological and Environmental Sciences, University of Bologna,

34   Piazza di Porta San Donato, I-40126 Bologna, Italy

35

36   * Corresponding author.

37

38

39

40

41

42

43

44

45

2

46

47   ABSTRACT

48

49   The direct carbonate procedure for AMS ^{14}C dating of sub-milligram samples of biogenic

50   carbonate without graphitization is becoming widely used in a variety of studies. We compare

51   the results of 153 paired direct carbonate and standard graphite ^{14}C determinations on single

52   specimens of an assortment of biogenic carbonates. An RMA regression shows a strong

53   relationship between direct carbonate and graphite percent Modern Carbon (pMC) values (m =

54   0.996; 95% CI (0.991 to 1.001)). An analysis of differences and a 95% confidence interval using

55   ±1σ analytical errors on pMC reveals that there is no significant difference between direct

56   carbonate and graphite pMC values for 76% of analyzed specimens, although variation in direct

57   carbonate pMC is underestimated. Offset between the two methods is typically within 2 pMC,

58   with 61% of the differences being positive. Of the 36 samples that did yield significant

59   differences, all but three missed the 95% significance threshold by 1.2 pMC or less. The

60   statistical disagreement in younger samples is driven by low analytical error, not increased

61   variability or bias. Direct carbonate ^{14}C dating of biogenic carbonates is a cost-effective and

62   efficient complement to standard graphite ^{14}C dating.

63

64   INTRODUCTION

65

66   An increasing variety of scientific investigations require a large number of radiocarbon analyses

67   to address their underlying research questions, as exemplified by recent studies assessing the

68   degree of time-averaging in natural or anthropological shelly accumulations (Kowalewski et al.,

69   2018; New et al., 2019, Parker et al., 2019; Albano et al., 2020). These studies are generally

70   constrained by their analytical budget rather than by the number of samples suitable for analysis,

71   whereas some are limited by the size of the targeted specimens. This is true for a variety of

72   sample types, including those based on biogenic carbonate. The traditional graphite AMS ^{14}C

73   technique requires 8 to 10 mg of carbonate, which excludes dating individual small bivalve

74   shells, for example. In response to this growing need, a direct carbonate AMS ^{14}C sputter

75   method was developed by Longworth et al. (2013) that allows sub-milligram samples of

76   carbonate powder to be analyzed quickly and efficiently. Several publications have highlighted

77   the utility of direct carbonate ^{14}C dating where it has been used on its own or in combination

78   with amino acid racemization to determine time-averaging in taphonomic studies (Dominguez et

79   al., 2016; Kosnik et al., 2017; Ritter et al., 2017; Parker et al., 2019; Albano et al., 2020) or

80   coupled with standard precision ^{14}C and uranium/thorium dating to determine coral age

81   distributions (Grothe et al., 2016).

82

83   The direct carbonate AMS ^{14}C technique uses a cesium sputter source and a metal powder as a

84   catalyst without the need to convert the carbonate sample to graphite, but yields beam currents

85   about an order of magnitude lower than the graphite method (Bush et al., 2013; Hua et al., 2019)

86   which leads to the lower precision. Longworth et al. (2013) analyzed several materials with

87   percent modern carbon (pMC) between 0.25 and 94.21. Using titanium powder, the method

88   produced 1σ errors that ranged from 0.07 and 0.94 pMC, whereas 1σ errors on the same

89   materials ranged from 0.08 and 0.87 pMC using graphite. Bush et al. (2013) analyzed numerous

90   coral samples containing 0.10 to 89.06 pMC. Using iron powder, the method produced 1σ errors

91   that ranged from 0.31 and 0.62 pMC, whereas 1σ errors on the same materials ranged from 0.03

4

92   and 0.11 pMC using graphite. Subsequent study by Hua et al. (2019) further established the

93   utility of the direct carbonate technique, testing iron (Fe), niobium (Nb), and silver (Ag) powders

94   before concluding that niobium powder was superior because it produced the highest beam

95   current and lowest background. Smith et al. (2010) showed a strong positive relationship

96   between carbon/Fe (µg/mg) and beam currents ($R^2 = 0.84$). If the amount of carbonate powder

97   and Nb or Fe powder in a target are the same, then the number of Nb ion present is about 60%

98   that of Fe. Therefore, the carbon/metal ion ratio is higher when using Nb, which may explain the

99   higher beam currents of direct carbonate ^{14}C determinations that use Nb powder.

100

101   Several studies have compared small numbers of paired direct carbonate and graphite ^{14}C results,

102   showing that the two methods are comparable (Bush et al., 2013; Kosnik et al., 2017;

103   Kowalewski et al., 2018; Hua et al., 2019, New et al., 2019; Albano et al., 2020). In this paper,

104   we have compiled a comprehensive dataset (n = 153) of published and unpublished direct

105   carbonate and graphite ^{14}C determinations from biogenic carbonates belonging to several

106   taxonomic groups (mollusks, corals, echinoderms, brachiopods) to further quantify any bias in

107   the results based on the direct carbonate method.

108

109   MATERIALS AND METHODS

110

111   The carbonates featured in this study are all biogenic, as opposed to inorganically precipitated

112   carbonate (e.g., limestone, speleothems). Samples comprise primarily aragonitic valves from the

113   clams *Arctica islandica* (Linnaeus, 1767), *Chamelea gallina* (Linnaeus, 1758), *Codakia*

114   *orbicularis* (Linnaeus, 1758), *Corbula gibba* (Olivi, 1792), *Dosinia caerulea* (Reeve, 1850),

5

115   *Mactra isabelleana* d'Orbigny, 1846, *Mulinia edulis* (King, 1832), *Tawera spissa* (Deshayes,

116   1835), *Tucetona pectinata* (Gmelin, 1791), from open nomenclature species of the clams

117   *Timoclea* and *Transennella*, from shells of the terrestrial snails *Actinella nitidiuscula* (Sowerby,

118   1824) and *Polygyra septemvolva* Say, 1818, and from skeletal material of unidentified corals. As

119   for the calcite polymorph, samples include valves from the brachiopod *Gryphus vitreus* (Born,

120   1778) and plates from the sand dollars *Peronella peronii* (Agassiz, 1841) and *Leodia*

121   *sexiesperforata* (Leske, 1778). Several samples are shells that contain a mixture of aragonite and

122   calcite polymorphs. These are the gastropods (limpets) *Fissurella maxima* Sowerby, 1834 and

123   *Patella candei* d'Orbigny 1840, the mussel *Choromytilus chorus* (Molina, 1782), the cockle

124   *Fulvia tenuicostata* (Lamarck, 1819), the scallop *Argopecten purpuratus* (Lamarck, 1819), and

125   an open nomenclature species of the mussel *Modiolus*. References pertaining to the

126   mineralogical composition of the biogenic material used in this study are provided in the

127   Supplemental Information.

128

129   Ninety-three paired carbonate samples were processed at Northern Arizona University's (NAU)

130   Amino Acid Geochronology Lab (AAGL) and NAU's Center for Ecosystem Science and Society

131   (Ecoss) between 2015 and 2019. Most of the samples processed at NAU have been previously

132   published (Kosnik et al., 2017; Oakley et al., 2017; Ritter et al., 2017; Kowalewski et al., 2018;

133   Albano et al., 2020) and are detailed in the Supplemental Information.

134

135   Sample preparation at NAU followed protocols modified from Bush et al. (2013). Blanks,

136   standards, and unknowns were sonicated in deionized distilled water (DDI water; 16.7

137   Mohm*cm), rinsed three times with DDI water, leached with 2N ACS grade hydrochloric acid,

6

138   and then finally rinsed three times with DDI to remove surface contaminants before being dried

139   in a 50° C oven overnight. Samples for direct carbonate ^{14}C analysis were ground to a fine

140   powder using an agate mortar and pestle and manually mixed with 6.0 to 7.0 mg of metal powder

141   in pre-baked (3 hr at 500° C) Kimble borosilicate glass culture tubes (6 mm OD x 50 mm).

142   Samples processed at NAU before June 2018 were mixed with Fe powder (Alfa Aesar, -325

143   mesh, reduced, 98%) whereas samples processed after June 2018 were mixed with Nb powder

144   (Alfa Aesar Puratronic, -325 mesh, 99.99%), following a change from Fe to Nb powders at the

145   Keck Carbon Cycle AMS facility at the University of California , Irvine (UCI) in 2018.

146   Powdered carbonate sample masses ranged between 0.30 and 0.50 mg, which equates to 36 to 60

147   µg of carbon, respectively. The culture tubes were flushed with N_2 gas to reduce contamination

148   from atmospheric carbon and capped with Supelco plastic column caps (1/4" OD) until the

149   carbonate-metal powder mixture was pressed into targets.

150

151   Samples processed at NAU for standard graphite AMS ^{14}C analysis were graphitized at NAU's

152   Ecoss lab following UCI protocols (sites.uci.edu/keckams/protocols). An aliquot of 7 to 8 mg of

153   carbonate was placed in 13 x 75 mm BD Vacutainer plastic collection tubes and sealed with a

154   red/grey conventional stopper closure. Ambient atmosphere was removed via vacuum before a

155   small-bore needle was used to dispense 8 ml of ACS grade 85% phosphoric acid into each tube.

156   The tubes were placed in a heating block at 70° C until the effervescence stopped. The evolved

157   gas was removed via vacuum. Water vapor was removed by passing the gas through a mixture of

158   liquid nitrogen and ethanol at approximately -50° C. Carbon dioxide was condensed to a solid

159   using a liquid nitrogen bath and the remaining gasses were drawn off. The purified CO_2 was

7

160 converted to graphite by reaction with Fe powder (Alfa Aesar, -325 mesh, reduced, 98%) in a

161 hydrogen reducing environment at 550° C for 3 hr (Vogel et al., 1984).

162

163 The carbonate-metal or graphite-metal mixtures were pressed into pre-drilled (4.1 mm depth)

164 aluminum targets at 400 psi, rotated 90°, and pressed again at 400 psi. Direct carbonate targets

165 were pressed within 72 hr of powdering the first sample. The IAEA C1 blank and IAEA C2

166 standard were pressed on the same day they were powdered. Processing a direct carbonate ^{14}C

167 sample, from raw shell to a finished pressed target, typically takes about 25 minutes. In

168 comparison, processing a typical graphite ^{14}C sample, from raw shell to final pressed target,

169 typically takes about 60 minutes. The pressed targets were sent to UCI for AMS ^{14}C analysis

170 (Southon and Santos, 2007).

171

172 We compiled 60 additional paired determinations generated at UCI or the Australian Nuclear

173 Science and Technology Organisation (ANSTO) from Bush et al. (2011), New et al. (2019),

174 Parker et al. (2019), and Hua et al. (2019). The respective publications provide the lab

175 procedures and methods used for the additional paired determinations. Co-authors contributed all

176 unpublished ages and previously unreported supporting information from UCI and ANSTO.

177

178 Radiocarbon concentrations are given as percent of the Modern (pMC) standard following the

179 conventions of Stuvier and Polach (1977). Sample preparation backgrounds have been subtracted

180 based on measurements of ^{14}C-free calcite (IAEA C1) using an isotope mixing calculation

181 (Donahue et al., 1990). All graphite ^{14}C determinations have been corrected for isotopic

182 fractionation according to conventions of Stuvier and Polach (1977) with δ^{13}C values measured

8

183   on prepared graphite using the AMS spectrometer. These can differ from the $\delta^{13}C$ values of the

184   original material and are not provided.

185

186   Differences were calculated as "direct carbonate – graphite pMC", with errors calculated in

187   quadrature. The bivariate relationship between direct carbonate and graphite pMC values was

188   evaluated using a reduced major axis regression (RMA) analysis. Unlike the classic ordinary

189   least squares regressions (OLS), the RMA – also known as standardized major axis, geometric

190   mean regression, or model II regression – minimizes the residual variation across both axes, not

191   only the Y-axis, and hence accounts for measurement error in both axes (Quinn and Keough

192   2002, Smith 2009). The RMA regression avoids assumptions about the cause-and-effect between

193   direct carbonate and graphite pMC values (Smith, 2009). The PAST 4.03 statistical program

194   (Hammer et al., 2001) was used for the RMA with 95% bootstrapped confidence intervals [N =

195   1999].

196

197   RESULTS AND DISCUSSION

198

199   Blank (IAEA C1) and Holocene standard (IAEA C2) performance

200

201   Graphite ^{14}C analysis of NAU's marble blank (IAEA C1) yields 0.44 ± 0.25 pMC (n = 8). Direct

202   carbonate ^{14}C analysis of NAU's C1 blank yields 2.16 ± 0.42 pMC (n = 22) using Fe and $1.49 \pm$

203   0.67 pMC (n = 115) using Nb powder. Our direct carbonate blank results are similar to Hua et al.

204   (2019) who demonstrated that Nb powder yields cleaner blanks than either Fe or Ag powders.

205   The source of the direct carbonate ^{14}C contamination in the NAU blank is unclear but likely

9

206 stems from a variety of sources including, but not limited to, contamination during processing,

207 carbon contamination in both the metal powders and the C1 powder itself, and uptake from

208 atmospheric sources (Longworth et al., 2013). It is well known that powdered carbonate adsorbs

209 atmospheric CO_2 over several years (Gagnon and Jones, 1993) but it also rapidly adsorbs CO_2

210 after being baked at 500° C to oxidize indigenous and adsorbed carbon (Bush et al., 2013). A

211 small test conducted at NAU reveals that C1 powder mixed with Nb and stored in capped glass

212 ampules under N_2 and then pressed immediately, pressed after four days, and pressed after nine

213 days yields similar pMC (2.5 ± 0.4 (n = 2); 2.3 ± 0.3 (n = 4); 2.1 ± 0.2 (n = 2), respectively). A

214 subsequent test used a ^{14}C-dead *Rangia lecontei* (Conrad, 1853) shell from the Early and Middle

215 Pleistocene Brawley Formation (Kirby et al., 2007). Targets pressed immediately after

216 powdering and pressed after four and nine days storage under N_2 yielded similar pMC (1.7 ± 0.1

217 (n = 4); 1.6 ± 0.1 (n = 4); 1.8 ± 0.1 (n = 4), respectively). The small difference in pMC between

218 the C1 blank and the *R. lecontei* blank is within the range of analytical variability of our C1

219 blank, thus, we contend that the marble and mollusc shell powders do not behave differently

220 during processing. Neither set of blanks suggest that adsorption of atmospheric CO_2 during

221 processing is a significant source of contamination, unless it occurs almost instantaneously upon

222 powdering. As standard practice, all direct carbonate ^{14}C blanks and standards processed at NAU

223 are pressed into targets on the same day they are powdered. Unknowns are powdered, stored

224 under N_2, and pressed into targets within 72 hours. The metal powder itself is probably a larger

225 source of carbon contamination (Bush et al., 2013; Hua et al., 2019) than is adsorption of

226 atmospheric CO_2.

227

228   Graphite ^{14}C analysis of NAU's Holocene carbonate standard (IAEA C2) yields 40.52 ± 0.74

229   pMC (n = 7). The C2 standard is consistent with the consensus value within 1σ error ($41.14 \pm$

230   0.03 pMC; Rozanski et al., 1992). Direct carbonate ^{14}C analysis of NAU's C2 standard yields

231   41.30 ± 0.53 pMC (n = 25) using Fe powder and 40.71 ± 0.60 pMC (n = 114) using Nb powder.

232   Both values are consistent with the consensus value within 1σ error (41.14 ± 0.03 pMC;

233   Rozanski et al., 1992). The difference in mean pMC is likely due to the smaller number of C2

234   standards analyzed with Fe powder. Thus, there is evidence for extraneous young carbon

235   contamination for the C1 and *R. lecontei* blanks (see previous section), but not for the C2

236   standard. Recently, Hua et al. (2019) demonstrated that the ^{14}C level of carbon contamination at

237   ANSTO is similar to the C2 standard pMC. Thus, extraneous carbon contamination would be

238   detectible in the C1 blank, but not in the C2 standard.

239

240   Key differences between direct carbonate and graphite ^{14}C determination for biominerals

241

242   The traditional graphite ^{14}C processing involves dissolving biominerals in phosphoric acid

243   followed by converting the resultant CO_2 to graphite. Negatively charged carbon ions are

244   produced by sputtering a mixture of graphite and iron powder with cesium ions and then

245   extracting the negatively charged carbon ions using an electric potential (Longworth et al.,

246   2013). The direct carbonate ^{14}C method bypasses the graphitization process and uses cesium ions

247   and an electrical potential to extract negatively charged carbon ions directly from powdered

248   carbonate mixed with a metal powder.

249

250   The presence/absence of the acid dissolution step is a key difference between two methods, and

251   might have interesting implications regarding the sources of carbon measured by the two

252   methods. Various studies suggest that mollusk shells (and other biominerals) contain a few tenths

253   of a percent up to 5% by mass organic material, or "conchiolin" (Fremy, 1855), which is an

254   integral structural component within the biomineral (Galstoff, 1964; Keith et al., 1993; Cuif et

255   al., 2004; Zhang and Zhang, 2006; Hadden et al., 2019). It is unclear if the acid dissolution of a

256   biomineral during traditional graphite ^{14}C processing can liberate carbon from conchiolin.

257   Presumably, conchiolin would be an additional source of carbon present only in direct carbonate

258   ^{14}C determinations. A non-exhaustive literature search suggests that paired shell and conchiolin

259   ^{14}C ages (or ^{14}C activities) are similar (Berger et al., 1965; Burliegh, 1983; Haynes and Mead,

260   1987; Hadden et al., 2019). In some environments, however, organisms may preferentially

261   incorporate significant amounts of ^{14}C-dead carbon in their conchiolin that is not present in their

262   soft tissues or shell carbonate (Masters and Bada, 1977; Hadden et al., 2018). We cautiously

263   assume that small amounts of conchiolin in the biominerals featured in this study do not

264   significantly influence the direct carbonate pMC values, but the topic deserves additional study.

265

266   Direct carbonate versus graphite pMC determinations

267

268   We compiled pMC values from 153 individual carbonate specimens analyzed using both the

269   direct carbonate and graphite ^{14}C techniques. Seventy-eight and 75 direct carbonate targets used

270   Fe and Nb powder, respectively (Supplemental Information). Bush et al. (2013) concluded that

271   the direct carbonate ^{14}C technique is less reliable for their oldest coral samples (> 30 ka BP),

272   thus, their samples yielding ≤ 1.3 pMC using graphite are excluded in this comparison. One

273   sample of *Mactra isabelleana* powder yielded strongly dissimilar graphite (78.5 pMC) and direct

274   carbonate (105.7 pMC) results when analyzed seven months apart. Two samples of *Actinella*

275   *nitidiuscula* material also produced strongly dissimilar graphite (0.91 and 0.36 pMC) and direct

276   carbonate (2.0 and 2.5 pMC) results, respectively. The reason for the discrepancies is unclear.

277   All three samples used Fe powder in the direct carbonate ^{14}C determinations. Two of the samples

278   yield pMC values close to background and are therefore sensitive to contamination, and the third

279   sample yielded pMC showing bomb ^{14}C contamination when analyzed with the direct carbonate

280   technique whereas it did not when analyzed as graphite, thus, these three samples were excluded

281   from further discussion. The remaining 150 specimens yield graphite and direct carbonate pMC

282   values between 2.2 and 106.0 (Supplemental Information).

283

284   Notably, the 1σ pMC analytical errors associated with the direct carbonate ^{14}C technique are

285   typically two to eight times higher than for their graphite counterpart (Fig. 1A). There is a

286   moderately weak negative relationships between the magnitude of the relative 1σ analytical

287   errors and a sample's graphite pMC when using Fe (r = -0.62) and Nb (r = -0.17) in direct

288   carbonate ^{14}C analyses (Fig. 1B). With better counting statistics and less proportional

289   background interference, direct carbonate pMC measurements on young samples tend to be

290   indistinguishable from their graphite counterpart measurements as compared to older samples.

291

292   An RMA regression shows a strong relationship between direct carbonate and graphite pMC (n =

293   150) (Fig. 2A). The slope of an RMA regression line is defined as the standard deviation of the

294   y-axis values (direct carbonate pMC) divided by the standard deviation of the x-axis values

295   (graphite pMC). The y-intercept is defined by the regression line passing through the bivariate

296   centroid, or the point $(\bar{x},\bar{y})$, which here would be the mean of the graphite pMC values and the

297   mean of the direct carbonate pMC values, respectively. The RMA regression using our entire

298   compilation (Fig. 2A) yields a slope near 1.000 (0.996 ± 0.003; 95% bootstrapped CI [N = 1999]

299   of 0.991 to 1.001), and a y-intercept slightly above 0.00 (0.42; 95% bootstrapped CI [N = 1999]

300   of 0.15 to 0.67) (Fig. 1A). We observe slight differences in the RMA regression results when the

301   direct carbonate ^{14}C determinations using Fe and Nb are assessed individually (Figs. 2B and 2C).

302   Variability in the direct carbonate ^{14}C determinations using Fe powder is similar to that of their

303   graphitized counterparts (i.e., RMA slope of 0.999± 0.003; Fig. 2B). In contrast, the lower RMA

304   slope of 0.988 ± 0.006 for the Nb-graphite pairs (Fig. 2C) reveals that the direct carbonate [14]C

305   determinations using Nb powder yield pMC values that are slightly less variable than their

306   graphite counterparts. The difference in the Fe-only and Nb-only RMA regression slopes is small

307   and overlap at 2σ errors. Thus, we contend that the differences in pMC values between the direct

308   carbonate and graphite ^{14}C techniques is insignificant for most analytical goals.

309

310   The vast majority of direct carbonate pMC values are comparable to their graphite counterparts.

311   Seventy-seven percent of differences are ± 1.0 pMC, and 94% percent are ± 2.0 pMC. Overall,

312   we observe that 61% of differences are positive (Fig. 2A). When considered individually,

313   however, 69% of the direct carbonate ^{14}C determinations using Fe yield positive differences

314   whereas the direct carbonate ^{14}C determinations using Nb yield differences that are more equally

315   distributed, but still with a slight positive skew (53%) (Figs. 2B and 2C). The mean value of the

316   differences is 0.19 pMC (95% CI: 0.04 to 0.34 pMC) for the entire compilation, indicating that

317   the direct carbonate ^{14}C technique yields pMC values slightly higher than the graphite technique.

318   Much of the offset in contained in the direct carbonate determinations using Fe powder,

14

319   however. When considered individually, the mean value of the Fe-graphite differences is 0.26

320   pMC (95% CI: 0.06 to 0.46 pMC), whereas the mean of the Nb-graphite differences is roughly

321   half that, at 0.11 pMC (95% CI: -0.23 to 0.34 pMC). Dividing the differences by the direct

322   carbonate pMC value yields a coefficient of variation of 0.9% (95% CI: -0.65% to 1.58%) for the

323   entire compilation. When considered individually, the coefficient of variation for the Fe and Nb

324   differences are 1.6% (95% CI: 0.3% to 2.8%) and 0.3% (95% CI: -0.3% to 0.6%) respectively.

325   Collectively, this reveals a slight positive bias in direct carbonate ^{14}C measurements relative to

326   the graphite technique, with a more pronounced bias when using Fe powder.

327

328   The reason for the positively skewed differences (Fig. 2A, Fig. 2B) and for why the two metal

329   powders perform differently is unclear. One potential explanation is the adsorption of young

330   atmospheric CO_2 during the powdering process (e.g., Kosnik et al., 2017). However, adsorption

331   of CO_2 reasonably should affect all of the biomineral powders similarly, and not show a

332   preference for the samples using Fe powder. Kosnik et al. (2017) suggested that perhaps the

333   blank (marble) powder adsorbs CO_2 less efficiently than the biomineral powders, which would

334   lead to excess adsorbed atmospheric CO_2 influence on biomineral pMC after blank subtraction.

335   A blank under-correction of this sort should also affect the carbonate powders mixed with both

336   metals similarly, rather than preferentially affecting the carbonate powders mixed with Fe (Figs.

337   2B and 2C). Finally, we did not detect any adverse adsorption of atmospheric CO_2 in our blank

338   marble powder or on ^{14}C-dead mollusk shell powder after storage under N_2 for up to 9 days (see

339   previous discussion of blank performance). Thus, adsorption of CO_2 during powdering does not

340   adequately explain the higher tendency for positive differences when using Fe powder (Fig. 2B).

341   It is conceivable that the more equitable differences using Nb powder (Fig. 2C) is related to the

15

342   improved beam current and reduced uncertainties when using Nb powder (Hua et al., 2019). We

343   believe that our compilation is the largest of its kind, but it may still be too small to determine

344   the reason for the positive skew in differences when using Fe powder (Fig. 2B).

345

346   The majority of the individual differences in our compilation (76%) include 0 at 95% CI,

347   indicating there is no significant difference between the majority of paired direct carbonate and

348   graphite pMC values (Supplemental Information). However, 36 of the differences (24%) do not

349   meet this criterion. These differences are evenly split between direct carbonate ^{14}C

350   determinations using Fe powder (n = 19) and Nb powder (n = 17) (Table 1). Thirty-one of the 36

351   differences that do not include 0 are from samples that yield > 50 pMC as graphite, and the

352   remaining five come from samples that yield < 50 pMC as graphite (Table 1). All five of the

353   older samples yield differences that miss the 95% CI threshold by 0.5 pMC or less (Table 1). For

354   the younger samples, 28/31 of the differences miss the 95% CI threshold by less than 1.2 pMC.

355   The remaining three differences miss the 95% CI threshold by 1.3, 1.7, and 1.8 pMC (Table 1).

356

357   We acknowledge and caution that our study is limited to comparing the results of one direct

358   carbonate and one graphite ^{14}C analyses per individual biomineral specimen. Several of the

359   results complied from Bush et al. (2013) comprise multiple analyses per coral specimen, but the

360   overwhelming majority of our comparisons are based on single paired results (Supplemental

361   Information). We calculated the weighted mean of the graphite and direct carbonate ^{14}C values

362   (weighted by 1/variance) and determined the number of biomineral specimens with 1σ analytical

363   errors that overlapped the weighted mean. Ninety-three percent of the graphite pMC values

364   overlap the weighted mean (versus the expected 68%), but only 45% of the direct carbonate

16

365   pMC values do (versus the expected 68%). Thus, the reported uncertainty in the direct carbonate

366   ^{14}C determinations underestimates the actual variance. We also suspect that some of the

367   differences noted in this study may reflect slight variability between subsamples of a single

368   biomineral specimen. Future comparative studies would benefit from analyzing each specimen

369   multiple times with each AMS ^{14}C technique to more fully assess if there are statistically

370   significant differences between the two techniques. Researchers typically only date a biomineral

371   specimen once rather than multiple times, thus our study is more directly analogous to that

372   approach. Keeping in mind that the direct carbonate pMC variance is underestimated and that we

373   are using a single paired graphite and direct carbonate comparison per specimen, we contend that

374   our study shows that the differences between the direct carbonate and graphite ^{14}C techniques is

375   insignificant for most analytical goals.

376

377   We also observe a potentially interesting association between particular taxa and the differences

378   that do not include 0 at a 95% CI. For example, the clams *Arctica islandica* (6/6 analyses) and

379   *Modiolus* sp. (4/10 analyses), the sand dollar *Peronella peronii* (5/12 analyses), and the

380   brachiopod *Gryphus vitreus* (3/6 analyses) appear to be disproportionately affected (Tables 1 and

381   2). The cause of this pattern is unclear. Carbonate mineralogy can be excluded because both

382   aragonitic samples and calcitic samples populate the group (Table 1). Furthermore, some

383   differences from the same taxon do include 0 at a 95% CI, for example, the remaining 3/6

384   *Gryphus vitreus* shells (Table 2). Thus, neither the organism (in a broader taxonomic sense) nor

385   the carbonate mineralogy of the various skeletal materials is a satisfactory explanation. Using Fe

386   or Nb powder for direct carbonate ^{14}C analysis does not explain why some taxa seem more

387   affected than others (Table 1). The apparent patterns in Tables 1 and 2 may be an artifact of the

17

388   small sample sizes per taxon, but it may hint that taxonomy or perhaps environmental variables

389   specific to the habitat or life cycle of each taxon requires further consideration (e.g., Kosnik et

390   al., 2017; Hadden et al., 2018). Larger sample sizes and additional tests are needed to better

391   understand what may be causing differences between direct carbonate and graphite pMC

392   determinations.

393

394   To further explore the relationship between the direct carbonate and graphite ^{14}C methods, the

395   pMC differences shown in Figure 2A are plotted with respect to their respective taxonomic

396   classifications in Figure 3. As noted previously in our discussion, the direct carbonate pMC

397   values are more consistently higher than their graphite equivalents (Fig. 3). There are hints in

398   Figure 3 that some biogenic carbonates might be prone to producing direct carbonate pMC

399   values that are systematically offset from their graphite counterpart, although again, the sample

400   sizes per taxon are admittedly small (1 to 24 individuals). The metal powder used in the direct

401   carbonate ^{14}C technique again does not appear to be a controlling factor at the taxonomic level

402   (Fig. 3). Note that the brachiopod *Gryphus vitreus* yields exclusively negative differences using

403   Nb powder, the clams *Tucetona pectinata* and *Transennella* sp. yield exclusively positive

404   differences using Fe powder, and the echinoderm *Peronella peronii* yields positive differences in

405   nine of 11 analyses using Nb powder (Fig. 3). Additional work is need to determine whether the

406   perceived taxonomic differences are real, for example if different taxa or perhaps different shells

407   from different environments contain consistently different amounts of conchiolin with different

408   ^{14}C activities than the surrounding shell carbonate (Hadden et al., 2018), or whether the

409   perceived differences are merely an artefact of small sample sizes.

410

18

411 To summarize, we find that 114/150 (76%) of the direct carbonate pMC values in this

412 compilation are statistically indistinguishable from their paired graphite pMC values (i.e.,

413 differences include 0) at the 95% confidence interval, and of the 36 samples that are not, all but

414 three are less than 1.2 pMC beyond the 95% confidence threshold. All direct carbonate [14]C

415 determinations, even the three with the largest differences exceeding the 95% CI threshold, show

416 offsets from their graphite pMC values that are insignificant for most analytical goals. We can

417 confidently demonstrate that in the large majority of cases the direct carbonate ^{14}C technique

418 yields pMC values from a variety of biogenic carbonates that are indistinguishable to pMC

419 values produced using the more costly and time-intensive graphite ^{14}C technique. Additional

420 work is needed to better understand the origin of the increased uncertainty in the direct carbonate

421 ^{14}C determinations, but even with this uncertainty, the technique is appropriate for a wide range

422 of applications.

423

424 CONCLUSIONS

425

426 This study compared 153 individual biogenic carbonate samples from echinoderms, mollusks,

427 brachiopods and corals that have been dated using both direct carbonate and graphite [14]C

428 techniques. Three samples were excluded from discussion because their direct carbonate and

429 graphite pMC values were strongly discordant. The remaining 150 samples range from 2.2 to

430 106.0 pMC. The direct carbonate ^{14}C technique produces 1σ pMC errors that are primarily two

431 to 8 times higher than the associated graphite errors, and there is a weak negative correlation

432 between the magnitude of the 1σ error differences and a sample's graphite pMC value. Our

433 comparison of 150 paired direct carbonate and graphite ^{14}C determinations reveals a strong RMA

19

434   regression relationship between the two techniques (m = 0.996; 95% CI (0.991 to 1.001)), and

435   pMC values that are statistically indistinguishable from each other in 76% of the samples (at

436   95% CI). The variance in direct carbonate pMC values is underestimated, however. All but three

437   of the direct carbonate ^{14}C determinations in this study were within 1.2 pMC of the 95% CI

438   threshold of being statistically indistinguishable from their graphite equivalent. Some types of

439   biogenic carbonates appear to produce direct carbonate pMC values that are consistently offset

440   from their graphite values, but sample sizes are small and the paired pMC values still statistically

441   overlap in the vast majority of cases. The direct carbonate ^{14}C technique yields pMC values that

442   overwhelmingly are indistinguishable from the standard graphite ^{14}C technique, but with the

443   added benefit of more efficient laboratory preparation and processing.

444

445   ACKNOWLEDGEMENTS

446

461

462 REFERENCES

463

464 Agassiz L. 1841. Monographies d'Échinodermes vivans et fossiles. Échinites. Famille des

465 Clypéasteroides. 2 (Seconde Monographie). Des Scutelles. Neuchâtel, Switzerland, i-iv, 1-151,

466 pls 1-27.

467

468 Albano PG, Hua Q, Kaufman DS, Tomašových A, Zuschin M, Agiadi K. 2020. Radiocarbon

469 dating supports bivalve-fish age coupling along a bathymetric gradient in high-resolution

470 paleoenvironmental studies. Geology 48:589-593, doi:10.1130/G47210.1.

471

472 Berger R, Fergusson GJ, Libby WF, 1965. UCLA radiocarbon dates IV*. Radiocarbon 7:336-

473 371, doi:10.1017/S0033822200037310.

474

475 Born I. 1778. Index rerum naturalium Musei Cæsarei Vindobonensis. Pars I.ma. Testacea.

476 Verzeichniß der natürlichen Seltenheiten des k. k. Naturalien Cabinets zu Wien. Erster Theil.

477 Schalthiere. [1-40], 1-458, [1-82]. Vindobonae; (Kraus).

478

21

479 Burleigh R. 1983. Two radiocarbon dates for freshwater shells from Hierakonpolis:

480 Archaeological and geological implications. Journal of Archaeological Science 10:361-367,

481 doi:10.1016/0305-4403(83)90074-2.

482

483 Bush SL, Santos GM, Xu X, Southon JR, Thiagarajan N, Hines SK, Adkins JF. 2013. Simple,

484 rapid, and cost effective: a screening method for ^{14}C analysis of small carbonate samples.

485 Radiocarbon 55:631-640, doi:10.1017/S0033822200057787.

486

487 Conrad TA. 1853. Descriptions of new fossils shells of the United States. Journal of the

488 Academy of Natural Sciences of Philadelphia 2:273-276.

489

490 Cuif J-P, Dauphin Y, Berthet P, Jegoudez J. 2004. Associated water and organic compounds in

491 coral skeletons: Quantitative thermogravimetry coupled to infrared absorption spectrometry.

492 Geochemistry, Geophysics, Geosystems 5, Q11011, doi:10.1029/2004GC000783.

493

494 Cusack M, Parkinson D, Freer A, Perez-Huerta A, Fallick AE, Curry BB. 2008. Oxygen isotope

495 composition of *Modiolus modiolus* aragonite in the context of biological and crystallographic

496 control. Mineralogical Magazine 72:569-577.

497

498 d'Orbigny AD. 1834-1847. Voyage dans l'Amérique méridionale (le Brésil, la République

499 orientale de l'Uruguay, la République Argentine, la Patagonie, la République du Chili, la

500 République de Bolivia, la République du Pérou), exécuté pendant les années 1826, 1827, 1828,

501 1829, 1830, 1831, 1832 et 1833, 5(3):Mollusques: i-xliii, 1-758, lám 1-85. París/Estrasburgo.

502

503 d' Orbigny AD. 1839-1842. Mollusques, Echinodermes, Foraminifères et Polypiers recueillis

504 aux Iles Canaries par MM. Webb et Berthelot et décrits par Alcide d'Orbigny. Mollusques. 117

505 p., pl. 1-7, 7B (p. 1-24 [Aug. 1839], 25-48 [Sept. 1839], 49-72 [Oct-1839], 73-104 [Jan. 1840],

506 105-136 [Mar. 1840],137-143 [Apr. 1840], 145-152 [Aug. 1842] pl. 1 [Jul. 1836], 2 [Dec. 1836],

507 3 [May 1842], 4-5 [June 1840], 7 [May 1842], 6,7B [Aug. 1842]. Béthune, Paris.

508

509 Deshayes, GP, Milne-Edwards H. 1835. Histoire Naturelle des Animaux sans Vertèbres,

510 présentant les caractères généraux et particuliers de ces animaux, leur distribution, leurs classes,

511 leurs familles, leurs genres, et la citation des principales espèces qui s'y rapportent, par J.B.P.A.

512 de Lamarck. Deuxième édition, Tome sixième. Histoire des Mollusques. iv + 600 pp. J. B.

513 Baillière: Paris.

514

515 Dominguez JG, Kosnik MA, Allen AP, Hua Q, Jacob DE, Kaufman DS, Whitacre K. 2016.

516 Time-averaging and stratigraphic resolution in death assemblages and Holocene deposits:

517 Sydney Harbour's molluscan record. Palaios 31:564-575, doi:10.2110/palo.2015.087.

518

519 Donahue DJ, Linick TW, Jull AJ. 1990. Isotope-ratio and background corrections for accelerator

520 mass spectrometry radiocarbon measurements. Radiocarbon 32:135-142,

521 doi:10.1017/S00338222000040121.

522

523 Dubois, P. 2014. Calcification in echinoderms. In: Jangoux M, Lawrence JM, editors.

524 Echinoderm Studies 3. Rotterdam: Balkema. p. 109-178.

525

526   Fenger T, Surge D, Schone B, Milner N. 2007. Sclerochronology and geochemical variation in

527   limpet shells (*Patella vulgate*): A new archive to reconstruct coastal sea surface temperature.

528   Geochemistry Geophysics GeoSystems 8, Q07001, doi:10.1029/2006GC001488.

529

530   Flores, C., Gayo, E.M., Salazar, D., Broitman, B.R. 2018. δ^{18}O of *Fissurella maxima* as a proxy

531   for reconstructing Early Holocene sea surface temperatures in the coastal Atacama desert (25°S).

532   Palaeogeography, Palaeoclimatology, Palaeoecology 499:22-34,

533   doi:10.1016/j.palaeo.2018.03.031.

534

535   Fremy ME. 1855. Recherches chimiques sure les os. Annales de Chimie et de Physique 43:47-

536   107.

537

538   Gagnon AR, Jones GA. 1993. AMS-graphite target production methods at the Woods Hole

539   Oceanographic Institution during 1986-1991. Radiocarbon 35:301-310,

540   doi:10.1017/S0033822200064985.

541

542   Galstoff PS. 1964. The American Oyster *Crassostrea virginica* Gmelin. Fishery Bulletin of the

543   U.S. Fish and Wildlife Service 64, 480 p.

544

545   Gmelin JF. 1791. Vermes. In: Gmelin JF. (Ed.) Caroli a Linnaei Systema Naturae per Regna Tria

546   Naturae, Ed. 13. Tome 1(6). G.E. Beer, Lipsiae [Leipzig]. pp. 3021-3910.

547

24

548 Goetz AJ, Steinmetz DR, Griesshaber E, Zaefferer S, Raabe D, Kelm K, Irsen S, Sehrbrock A,

549 Schmahl WW. 2011. Interdigitating biocalcite dendrites for a 3-D jigsaw structure in brachiopod

550 shells. Acta Biomineralia 7:2237-2243, doi:10.1016/j.actbio.2011.01.035.

551

552 Grothe PR, Cobb KM, Bush SL, Cheng H, Santos G.M, Southon JR, Edwards RL, Deocampo

553 DM, Sayani HR. 2016. A comparison of U/Th and rapid-screen ^{14}C dates from Line Island fossil

554 corals. Geochemistry, Geophysics, Geosystems 17:833-845, doi:10.1002/2015GC005893.

555

556 Hadden CS, Loftis KM, Cherkinsky A. 2018. Carbon isotopes (δ^{13}C and Δ^{14}C) in shell

557 carbonate, conchiolin, and soft tissues in eastern oyster (*Crassostrea virginica*). Radiocarbon

558 60:1125-1137, doi:10.1017/RDC.2018.27.

559

560 Hadden, CS, Loftis KM, Cherinsky A, Ritchison BT, Lulewicz IH, Thompson, VD. 2019.

561 Radiocarbon in the marsh periwinkle (*Littorina irrorata*) conchiolin: applications for

562 archaeology. Radiocarbon 61:1489-1500, doi:10.1077/RDC.2019.53.

563

564 Hammer Ø, Harper DAT, Ryan PD. 2001. PAST: Paleontological statistics software package for

565 education and data analysis. Palaeontologia Electronica v. 4, no. 1, 9 pp.

566 http://palaeo-electronica.org/2001_1/past/issue1_01.htm. Accessed version 4.03, June 30, 2020.

567

568 Haynes CV, Jr, Mead AR. 1987. Radiocarbon dating and paleoclimatic significance of subfossil

569 Limicolaria in northwestern Sudan. Quaternary Research 28:86-99,

570 doi:10.1016/0033-5894(87)90035-4.

25

571

572   Hua Q, Lavchenko VA, Kosnik MA. 2019. Direct AMS ^{14}C analysis of carbonate. Radiocarbon

573   61:1431-1440, doi:10.1017/RDC.2019.24.

574

575   Jones CA. 2010. Mineralogy and seasonal growth of south Pacific mussel valves [MS thesis].

576   The University of Alabama, Tuscaloosa, Alabama, 73 pp.

577

578   Keith J, Stockwell S, Ball D, Remillard K, Kaplan D, Thannhauser T, Sherwood R. 1993.

579   Comparative analysis of macromolecules in mollusc shells. Comparative Biochemistry and

580   Physiology B 105:578-496, doi:10.1016/0305-0491(93)90078-J.

581

582   Kennedy WJ, Taylor JD, Hall A. 1969. Environmental and biological controls on bivalve shell

583   mineralogy. Biological Review 44:499-530.

584

585   King PP. 1832. Description of the Cirrhipeda, Conchifera and Mollusca, in a collection formed

586   by the officers of H.M.S. Adventure and Beagle employed between the years 1826 and 1830 in

587   surveying the southern coasts of South America, including the Straits of Magalhaens and the

588   coast of Tierra del Fuego. Zoological Journal 5: 332-349.

589

590   Kirby SM, Janecke SU, Dorsey RJ, Housen BA, Langenheim VE, McDougall KA, Steely AN.

591   2007. Pleistocene Brawley and Ocotillo Formations: Evidence for initial strike-slip deformation

592   along the San Felipe and San Jacinto Fault Zone, southern California. The Journal of Geology

593   115:43-62, doi:10.1086/509248.

594

595   Kosnik MA, Hua Q, Kaufman DS, Kowalewski M, Whitacre K. 2017. Radiocarbon-calibrated

596   amino acid racemization ages from Holocene sand dollars (*Peronella peronii*). Quaternary

597   Geochronology 39:174-188, doi:10.1016/j.quageo.2016.12.001.

598

599   Kowalewski M, Casebolt S, Hua Q, Whitacre KE, Kaufman DS, Kosnik MA. 2018. One fossil

600   record, multiple time resolutions: Disparate time-averaging of echinoids and mollusks in a

601   Holocene carbonate platform. Geology 46:51-54, doi:10.1130/G39789.1.

602

603   Lamarck J-BM de. 1819. Histoire naturelle des animaux sans vertèbres. Tome sixième, 1re

604   partie. Paris: published by the Author, vi + 343 pp.

605

606   Leske NG. 1778. Additamenta ad Jacobi Theodori Klein Naturalem Dispositionem

607   Echinodermatum et Lucubratiunculam de Aculeis Echinorum Marinorum. 216p.

608

609   Linnaeus C. 1758. Systema Naturae per regna tria naturae, secundum classes, ordines, genera,

610   species, cum characteribus, differentiis, synonymis, locis. Editio decima, reformata [10th revised

611   edition], vol. 1: 824 pp. Laurentius Salvius: Holmiae.

612

613   Linnaeus C. 1767. Systema naturae per regna tria naturae: secundum classes, ordines, genera,

614   species, cum characteribus, differentiis, synonymis, locis. Ed. 12. 1., Regnum Animale. 1 & 2.

615   Holmiae, Laurentii Salvii. Holmiae [Stockholm], Laurentii Salvii. pp. 1-532 [1766] pp. 533-1327

616   [1767].

617

618   Longworth BE, Robinson LF, Roberts ML, Beaupre SR, Burke A, Jenkins WJ. 2013. Carbonate

619   as a sputter target material for rapid ^{14}C AMS. Nuclear Instruments and Methods in Physics

620   Research B 294:328-334, doi:10.1016/j.nimb.2012.05.014.

621

622   Masters PM, Bada JL. 1977. Racemization of isoleucine in fossil molluscs from Indian middens

623   and interglacial terraces in southern California. Earth and Planetary Science Letters 37:173-183,

624   doi:10.1016/0012-821X(77)90162-5.

625

626   Molina DJI. 1782. Compendio de la historia geografica natural y civil del Reyno de Chile.

627   Premiera parte. Madrid. 418 pp.

628

629   New E, Yanes Y, Cameron RAD, Miller JH, Teixeira D, Kaufman DS. 2019. Aminochronology

630   and time averaging of Quaternary land snail assemblages form colluvial deposits in the Madeira

631   Archipelago, Portugal. Quaternary Research 92:483-496, doi:10.1017/qua.2019.1.

632

633   Nielsen JK, Helama S, Rodland D, Nielsen JK. 2007. Eemian marine mollusks and barnacles

634   from Ristinge Klint, Denmark: hydrodynamics and deficiency. Netherlands Journal of

635   Geoscience 86:95-115.

636

637 Oakley DOS, Kaufman DS, Gardner TW, Fisher DM, VanderLeest RA. 2017. Quaternary

638 marine terrace chronology, North Canterbury, New Zealand, using amino acid racemization and

639 infrared-stimulated luminescence. Quaternary Research 87:151-167, doi:10.1017/qua.2016.9.

640

641 Olivi G. 1792. Zoologia Adriatica, ossia catalogo ragionato degli animali del golfo e della lagune

642 di Venezia. Bassano [G. Remondini e fl.]. [ix] + 334 + xxxii pp., 9 pls.

643

644 Parker WG, Yanes Y, Hernández EM, Hernández Marreno JC, Paris J, Surge D. 2019. Scale of

645 time-averaging in archaeological shell middens from the Canary Islands. The Holocene 1-14,

646 doi:10.1177/0959683619883020.

647

648 Paul D, Mauldin R. 2013. Implications for Late Holocene climate from stable carbon and oxygen

649 isotopic variability in soil and land snail shells from archaeological site 41KM69 in Texas, USA.

650 Quaternary International 308-309:242-252, doi:10.1016/j.quaint.2012.08.006.

651

652 Quinn GP, Keough MJ. 2002. Experimental design and data analysis for biologists. Cambridge

653 University Press, Cambridge, UK. 537 pp.

654

655 Reeve LA. 1850. Monograph of the genus *Artemis* . pp. pls 1-10 in Reeve LA. Conchologia

656 Iconica. London : L. Reeve & Co. Vol.6.

657

29

658 Ritter MN, Erthal F, Kosnik MA, Coimbra JC, Kaufman DS. 2017. Spatial variation in the

659 temporal resolution of subtropical shallow-water molluscan death assemblages. Palaios 32:572-

660 583, doi:10.2110/palo.2017.003.

661

662 Roger LM, George, AD, Shaw J, Hart, RD, Roberts M, Becker T, McDonald BJ, Evans, NJ.

663 2017. Geochemical and microstructural characterization of two species of cool-water bivalves

664 (*Fulvia tenuicostata* and *Soletellina biradiata*) from Western Austraila. Biogeosciences 14:1721-

665 1737, doi:10.5194/bg-14-1721-2017.

666

667 Rozanski K, Stichler W, Gofiantini R, Scott EM, Beukens RP, Kromer B, Van Der Plicht J.

668 1992. The IAEA [14]C Intercomparison Exercise 1990. Radiocarbon 34:506-519,

669 doi:10.17/S0033822200063761.

670

671 Say T. 1818. Account of two new genera, and several new species, of fresh water and land

672 snails. Journal of the Academy of Natural Sciences of Philadelphia 1: 276-284.

673

674 Smith RJ. 2009. Use and misuse of the reduced major axis for line-fitting. American Journal of

675 Physical Anthropology 140:476-486, doi:10.1002/ajpa.21090.

676

677 Smith AM, Hua Q, Williams A, Levchenko V, Yang B. 2010. Developments in micro-sample

678 ^{14}C AMS at the ANTARES AMS facility. Nuclear Instruments and Methods in Physics Research

679 B 238:919-912, doi:10.1016/j.nimb.2009.10.064.

680

681   Southon J, Santos GM. 2007. Life with MC-SNICS. Part II: Further ion source development at

682   the Keck Carbon Cycle AMS Facility. Nuclear Instruments and Methods in Physics Research B

683   259:88-93, doi:10.1016/j.nimb.2007.01.147.

684

685   Sowerby, GB, I. 1824. Descriptions, accompanied by figures, of several Helices, discovered by

686   T. E. Bowdich, Esq. at Porto Santo. Zoological Journal 1: 56-58 [March].

687

688   Sowerby GB., I; Sowerby, GB, II. 1832-1841. The conchological illustrations or, Coloured

689   figures of all the hitherto unfigured recent shells. London, privately published.

690

691   Stuvier M, Polach HA. 1977. Discussion reporting of ^{14}C data. Radiocarbon 19:355-363,

692   doi:10.1017/S0033822200003672.

693

694   Tschudin P. 2001. Shell morphology, shell texture and species discrimination of Caribbean

695   *Tucetona* (Bivalvia, Gylcymeridae). Journal of Paleontology 75:658-679.

696

697   Vogel, JS, Southon, JR, Nelson, DE, Brown, TA. 1984. Performance of catalytically condensed

698   carbon for use in accelerator mass spectrometry. Nuclear Instruments and Methods in Physics

699   Research 223:289-293.

700

701   Yanes Y, Al-Qattan NM, Rech JA, Pigati JS, Dodd JP, Nedila JC. 2019. Overview of the oxygen

702   isotope systematics of land snails from North America. Quaternary Research 91:329-344,

703   doi:10.1017/qua.2018.79.

31

704

705   Zhang C, Zhang R. 2006. Matrix proteins in the outer shells of Molluscs. Marine Biotechnology

706   8:572-586, doi:10.1007/s10126-005-6029-6.

707

708   FIGURE CAPTIONS

709

710   Figure 1. Cross-plots comparing analytical errors for direct carbonate and graphite pMC from the

711   same biogenic carbonates. A - cross-plot of 1σ analytical errors produced by the graphite [14]C

712   method versus the 1σ analytical errors produced by the direct carbonate ^{14}C method. Dashed line

713   is a 1-to-1 line. B - cross-plot of graphite pMC versus the ratio of direct carbonate to graphite 1σ

714   pMC analytical errors. Moderate negative correlations are defined by the coarse (Fe; r = -0.62)

715   and fine (Nb; r = -0.17) dashed lines. Solid black circles in both panels – Fe powder. Solid white

716   circles in both panels – Nb powder.

717

718   Figure 2. Reduced Major Axis (RMA) regression of paired direct carbonate and graphite pMC

719   determinations. A –relationship using all data. B – relationship using iron (Fe) powder. C –

720   relationship using niobium (Nb) powder. Analysis performed using PAST 4.03 statistical

721   software (Hammer et al., 2001). Inset diagrams are frequency histograms of pMC differences,

722   calculated as "direct – graphite pMC".

723

724   Figure 3. Differences in pMC (direct carbonate – graphite) from an assortment of biogenic

725   carbonates. Bp -brachiopod, G – gastropod, E – echinoderm, B – bivalve mollusk. Note that most

726   differences are positive and that some biogenic carbonates more consistently yield either

32

727   negative (e.g., *Gryphus vitreus*) or positive (e.g., *Transennella* sp.) differences, while others are

728   more evenly distributed (e.g., *Dosinia caerulea*, coral skeletons). See Supplemental Information

729   for additional information on taxonomy and carbonate polymorphs. Solid black circles– Fe

730   powder. Solid white circles – Nb powder.

731

732

733

734

735

736

737

738

739

740

741

742

743

744

745

746

747

748

749

750 Table 1 Detailed breakdown of the taxa, generalized biological group, carbonate polymorph,
751 standard graphite pMC values, direct carbonate metal powder, and absolute pMC value of
752 individual differences that exclude 0 at 95% CI.
753

Taxon	Group	Polymorph	Graphite pMC	Direct carbonate powder	Absolute pMC beyond 95% CI
Actinella nitidiuscula	snail	aragonite	10.9	Nb	0.53
Argopecten purpuratus	scallop	mixed	68.9	Fe	0.18
Argopecten purpuratus	scallop	mixed	70.5	Fe	0.10
Arctica islandica	clam	aragonite	50.5	Fe	0.89
Arctica islandica	clam	aragonite	50.9	Fe	0.65
Arctica islandica	clam	aragonite	51.4	Fe	0.13
Arctica islandica	clam	aragonite	55.5	Fe	0.07
Arctica islandica	clam	aragonite	74.0	Fe	1.80
Arctica islandica	clam	aragonite	75.3	Fe	0.11
Codakia orbicularis	clam	aragonite	103.3	Fe	0.70
Codakia orbicularis	clam	aragonite	103.3	Fe	1.72
unidentified coral	coral	aragonite	2.6	Fe	0.25
Corbula gibba	clam	aragonite	94.7	Nb	1.30
Dosinia caerulea	clam	aragonite	66.5	Nb	0.26
Dosinia caerulea	clam	aragonite	77.2	Nb	0.35
Fissurella maxima	limpet	mixed[a]	28.3	Nb	0.08
Fissurella maxima	limpet	mixed[a]	48.8	Nb	0.07
Gryphus vitreus	brachiopod	calcite	76.1	Nb	0.24
Gryphus vitreus	brachiopod	calcite	87.4	Nb	0.29
Gryphus vitreus	brachiopod	calcite	88.9	Nb	0.36
Leodia sexiesperforata	echinoderm	calcite	104.9	Fe	0.30
Modiolus sp.	mussel	aragonite	52.3	Fe	0.14
Modiolus sp.	mussel	aragonite	61.6	Fe	0.04
Modiolus sp.	mussel	aragonite	76.1	Fe	0.45
Modiolus sp.	mussel	aragonite	79.4	Fe	0.32
Mulinia edulis	clam	aragonite	93.2	Fe	0.38
Patella candei	limpet	mixed[a]	77.2	Nb	0.25
Patella candei	limpet	mixed[a]	88.1	Nb	0.19
Peronella peronii	echinoderm	calcite	57.0	Nb	1.01
Peronella peronii	echinoderm	calcite	62.1	Nb	1.17
Peronella peronii	echinoderm	calcite	72.4	Nb	1.17
Peronella peronii	echinoderm	calcite	77.2	Nb	0.83
Peronella peronii	echinoderm	calcite	77.7	Nb	1.15
Polygyra septemvolva	snail	aragonite	33.0	Nb	0.43
Transennella sp.	clam	aragonite	77.2	Fe	0.06
Tucetona pectinata	clam	aragonite	59.0	Fe	0.06

754 [a] "mixed" refers to shells that contain both calcite and aragonite polymorphs.
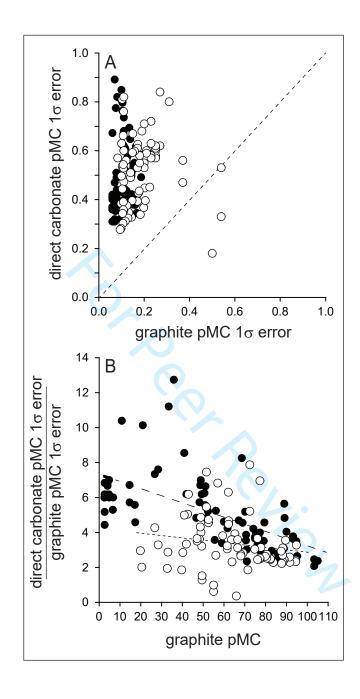
755

756

757 Table 2 Summary of the taxa, sample size (n), generalized biological group, carbonate
758 polymorph, number of differences that include 0 at 95% CI, and publication information for
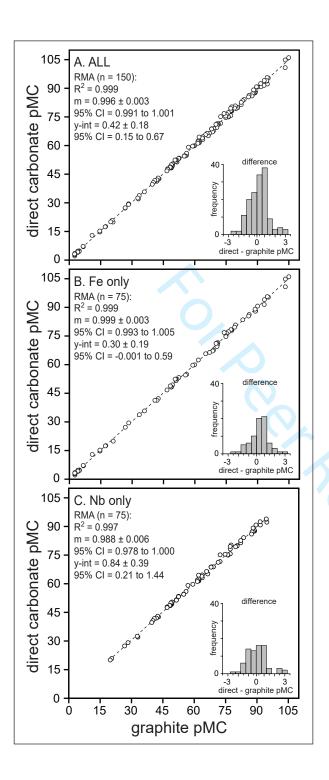759 samples featured in this study.
760

Taxon	n	Group	Polymorph	Residuals include 0	Reference
Actinella nitidiuscula	6[a]	snail	aragonite	3/4	New et al. (2019)
Argopecten purpuratus	5	scallop	mixed	3/5	this study
Arctica islandica	6	clam	aragonite	0/6	this study
Chamelea gallina	1	clam	aragonite	1/1	this study
Choromytilus chorus	12	mussel	mixed[b]	12/12	this study
Codakia orbicularis	6	clam	aragonite	4/6	this study
unidentified coral	20	coral	aragonite	19/20	Bush et al. (2011)
Corbula gibba	3	clam	aragonite	2/3	Albano et al. (2020)
Corbula gibba	2	clam	aragonite	2/2	this study
Dosinia caerulea	24	clam	aragonite	22/24	this study
Fissurella maxima	10	limpet	mixed[b]	8/10	this study
Fulvia tenuicostata	8	cockle	mixed[b]	8/8	Hua et al. (2019)
Gryphus vitreus	6	brachiopod	calcite	3/6	this study
Leodia sexiesperforata	1	echinoderm	calcite	0/1	Kowalewski et al. (2018)
Mactra isabelleana	1[a]	clam	aragonite	0/1	Ritter et al. (2017)
Modiolus sp.	10	mussel	aragonite	6/10	this study
Mulinia edulis	5	clam	aragonite	4/5	this study
Patella candei	5	limpet	mixed[b]	3/5	Parker et al. (2019)
Peronella peronii	11	echinoderm	calcite	6/11	Kosnik et al. (2017)
Polygyra septemvolva	2	snail	aragonite	1/2	this study
Tawera spissa	1	clam	aragonite	1/1	Oakley et al. (2017)
Timoclea sp.	1	clam	aragonite	1/1	this study
Transennella sp.	4	clam	aragonite	3/4	this study
Tucetona pectinata	3	clam	aragonite	2/3	Kowalewski et al. (2018)

761 [a] Two analyses of *Actinella nitidiuscula* and one analysis of *Mactra isabelleana* yield widely
762 different direct carbonate and graphite pMC values and are excluded from discussion and
763 statistical analysis. See Supplemental Information.
764 [b] "mixed" refers to shells that contain both calcite and aragonite polymorphs.

A. ALL
RMA (n = 150):
$R^2 = 0.999$
m = 0.996 ± 0.003
95% CI = 0.991 to 1.001
y-int = 0.42 ± 0.18
95% CI = 0.15 to 0.67

B. Fe only
RMA (n = 75):
$R^2 = 0.999$
m = 0.999 ± 0.003
95% CI = 0.993 to 1.005
y-int = 0.30 ± 0.19
95% CI = -0.001 to 0.59

C. Nb only
RMA (n = 75):
$R^2 = 0.997$
m = 0.988 ± 0.006
95% CI = 0.978 to 1.000
y-int = 0.84 ± 0.39
95% CI = 0.21 to 1.44

direct carbonate -
graphite pMC